Colloids and Surfaces A: Physicochemical and Engineering Aspects 702 (2024) 134970

Contents lists available at ScienceDirect

Colloids and Surfaces A: Physicochemical and Engineering Aspects

journal homepage: www.elsevier.com/locate/colsurfa

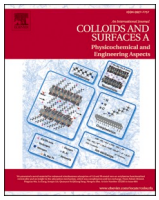

Interactions of polychlorinated cyclodiene pesticides with model fungal membranes – Langmuir monolayer and liposome studies

Marcin Broniatowski [a,*], Aneta Wójcik [a,b], Mareike S. Stephan [b], Vasil N. Georgiev [b], Rumiana Dimova [b], Marzena Mach [c], Paweł Wydro [c]

[a] Department of Environmental Chemistry, Faculty of Chemistry, the Jagiellonian University in Kraków, ul-Gronostajowa 2, Kraków 30-387, Poland
[b] Max Planck Institute of Colloids and Interfaces, Science Park Golm, Potsdam 14476, Germany
[c] Department of Physical Chemistry and Electrochemistry, Faculty of Chemistry, the Jagiellonian University in Kraków, ul. Gronostajowa 2, Kraków 30-387, Poland

HIGHLIGHTS

- Cyclodiene pesticides are incorporated into model fungal membranes
- Cyclodiene pesticides do not disturb the formation of phospholipid crystalline nanodomains
- Chlordecone has the greatest impact on the physical properties of Langmuir monolayers
- All studied cyclodiene pesticides fluidize the lipid bilayer in liposomes

GRAPHICAL ABSTRACT

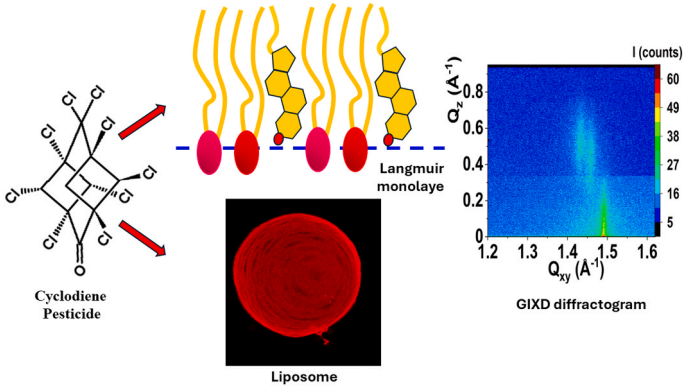

ARTICLE INFO

Keywords:
Cyclodiene pesticides
Model fungal membranes
Langmuir monolayers
Liposomes
Phospholipids
Grazing incidence X-ray diffraction

ABSTRACT

Polychlorinated cyclodiene pesticides (CP) are persistent organic pollutants causing widespread soil contamination. CPs-contaminated soils could be purified by mycoremediation, i.e. the introduction of CP-degrading fungal strains into the soils. However, not all mycoremediation attempts are effective, and the microbial cells introduced into the soil die. CP molecules are highly hydrophobic, therefore, their toxicity may largely result from membrane activity, i.e. from the incorporation of CP molecules into membranes disturbing their functions. To test this hypothesis and shed light on the interactions of CPs with plasma membranes, we used lipid Langmuir monolayers and unilamellar liposomes as models of fungal membranes. In our research, we included the four most common CPs polluting soils: aldrin, endrin, endosulfan, and chlordecone. Our studies have shown that CPs can be incorporated into the membranes up to the molar ratio of approximately 0.15. In the case of Langmuir monolayers, greater effects were observed for the model composed of saturated lipids. For this model, however, X-ray diffraction studies have shown that CPs are incorporated into the ergosterol-enriched amorphous phase without disturbing the formation of crystalline phospholipid nanodomains. Langmuir monolayer studies showed that chlordecone disturbs the physical properties of the model membrane to the greatest extent. However,

* Corresponding author.
E-mail address: broniato@chemia.uj.edu.pl (M. Broniatowski).

https://doi.org/10.1016/j.colsurfa.2024.134970
Received 18 June 2024; Received in revised form 17 July 2024; Accepted 30 July 2024
Available online 31 July 2024

liposome studies have shown that the effect of all CPs is similar – their presence increases the fluidity of the bilayer. Our studies confirmed CPs' membrane activity, however, also showed that the presence of CP molecules in lipid membranes does not cause drastic changes in their physical properties.

1. Introduction

The development of effective soil remediation techniques is one of the most important challenges of contemporary environmental chemistry [1–4]. This is not an easy challenge as soils can accumulate virtually any contaminants, from heavy metals [5–7] through petroleum hydrocarbons [8] to persistent organic pollutants (POP) [9–11]. Among POPs, polychlorinated pesticides, especially polychlorinated cyclodiene pesticides, are particularly dangerous contaminants.

Cyclodiene pesticides (CP) were introduced to the American market in the late forties of the previous century [12,13]. The precursor of these compounds is hexachlorocyclopentadiene which is subjected to the Diels-Alder reaction with different cyclic dienophiles [14]. CPs were very effective against multiple insects, however, soon after their first applications they were found very toxic to non-target animals, including humans [13,15]. CPs are very persistent in the environment [16], and due to their hydrophobicity easily migrate to adipose tissue, which leads to their biomagnification in trophic chains [17]. Some CPs, such as aldrin (ALD) or endrin (END) were banned in the USA already in the seventies of the 20th century, but other more polar derivatives, such as endosulfan (EDS) [18] or chlordecone (CDN) [19] were still in usage in the first decade of the 21st century and are still locally applied in some developing countries.

Due to their hydrophobicity, very low water solubility, and limited biodegradation, CPs accumulate in soils leading to the persistent pollution of vast areas [11,20]. Due to the high dispersion in the soil, CPs are a problematic carbon source for bacteria [21], resulting in a reduced efficiency of bacterial remediation of CP-polluted soil. The alternative can be the application of soil fungi [22–24]. The rapidly growing hyphae of mycelium can penetrate aerial voids in the soil, overgrow the organic detritus and humic matter, and often degrade different POPs absorbed therein, including CPs [22]. On the other hand, CPs can also be toxic to soil fungi, which is associated with the membrane-disruptive activity of these substances [24,25]. The fungal metabolism of the hydrophobic persistent pollutants is membrane-dependent [22,26] and the accumulation of chlorinated pesticides in the membranes can be the main reason for their toxicity toward soil fungi [27–29].

Soils can be in-situ actively purified of POP in many ways. Soils ca be enriched with various sorbents, such as biochar [30] or fertilizers containing appropriately designed nanoparticles [2,31,32]. Another approach is bioaugmentation, i.e. introducing organic pollutants degrading microorganisms directly into the soils [33]. Soil fungi can be effectively applied in the remediation of CP-polluted soil, which can be achieved both ex-situ in bioreactors and in-situ in field conditions [16, 18,34–38]. Thus, multiple examples of effective fungal bioaugmentation of soils polluted by PAHs or CPs were previously described [39–43]. However, it was highlighted that the success of such bioaugmentation cannot be predicted *a-priori*, as it depends on the concentration of the pollutants, their distribution in the soils, and especially on the fungal species applied for bioaugmentation [44–46]. In many cases, the toxicity of the POP molecules prevailed leading to limited growth of the mycelium and finally death of the fungus.

The laboratory and field bioremediation studies can be supported by laboratory experiments focusing on POP molecules' interactions with a fungal plasma membrane model [28,29,47]. Such studies can elucidate the questions regarding the membrane toxicity of a particular pollutant or correlate the composition of the model membrane with the effects triggered by the incorporation of the pollutant molecules into the studied membrane [47,48]. Finally, the results of such model studies can greatly help implement large-scale bioaugmentation and limit the number of unsuccessful cases. Therefore, in our studies, we created models of fungal plasma membranes and examined the impact of the incorporation of small amounts of cyclodiene pesticides on their physical properties, and crystalline structure. We employed lipid Langmuir monolayers, large unilamellar vesicles (LUV), and giant unilamellar vesicles (GUV) as model membranes. The combination of mutually complementary models, representing the membrane behavior of nanometer and cell-size scales, enabled the studies of different membrane characteristics. The employment of Langmuir monolayers allowed the study of the effects of CP incorporation on membrane condensation and 2D crystalline packing on the molecular scale. LUV and GUV studies investigated the effects of CP incorporation on the bilayer fluidity and stiffness. The plasma membrane composition and its dependence on environmental conditions for the most widespread soil fungi, namely *Aspergillus*, *Penicillium*, and *Fusarium* were previously described by others [49–51]. We made an informed choice for the composition of the fungal membrane based on published data and our previous studies [47, 52]. We tested four representatives of CPs: aldrin, endrin, endosulfan, and chlordecone, as these pesticides are most commonly identified as soil pollutants of the CP group. All four CP pesticides are listed in Annex A of the Stockholm Convention [9], as typical POP of global concern. Thus, understanding their interactions with soil microorganisms and further developing techniques for their elimination from the soil is highly required.

2. Experimental

2.1. Chemicals

All the phospholipids employed in the studies: 1-palmitoyl-2-oleoyl-sn-glycero-3-phosphoethanolamine (POPE), 1,2-dipalmitoyl-sn-glycero-3-phosphoethanolamine (DPPE), 1-palmitoyl-2-oleoyl-glycero-3-phosphocholine (POPC), 1,2-dipalmitoyl-sn-glycero-3-phosphocholine (DPPC), and ergosterol were purchased from Avanti Polar Lipids. Organic solvents of HPLC grade, chloroform, and methanol were bought from Merck Sigma Aldrich. Analytical standards of the studied cyclodiene pesticides: aldrin (ALD), endrin (END), endosulfan (EDS), and chlordecone (CDN) were also purchased from Merck Sigma Aldrich. The structural formulae of these molecules are shown in Scheme 1. Ultrapure water with a resistivity of 18.2 MΩ·cm was produced in our laboratory with the application of the Merck MilliPore water purification system.

3. Model membranes

Samples of lipids and pesticides were weighed on a Mettler Toledo balance with the accuracy of 10 μg and dissolved in chloroform/methanol 9/1 v/v mixture. The concentrations of pesticide solutions were of the order of 0.1 mg/ml, whereas those of the lipids were 0.2–0.3 mg/ml. All the stock solutions were stored at – 20 °C. Appropriate volumes of the stock solutions were mixed in dark glass vials just before the experiments to achieve the required composition of the components in the studied systems.

Information about the composition of the plasma membrane of different soil fungi has been reported previously [47–52]. Generally, the two main phospholipid classes in these membranes are phosphatidylcholines (PC) and phosphatidylethanolamines (PE), constituting usually 80 % of all phospholipids. The remaining 20 % are mainly phosphatidylserines (PS) and phosphatidylinositols (PI). The key lipid in fungal membranes is ergosterol, the content of which depends on the fungal species, the development stage of the hyphae, and the environmental

conditions and usually ranges between 10 and 50 mol% of all membrane polar lipids [50,53]. The saturation of the lipid acyl chains depends also on the fungal species and environmental conditions, but four fatty acids, two saturated 16:0, and 18:0, and two unsaturated 18:1, and 18:2 dominate [50,54,55]. Typically, the saturated chain is substituted in the sn1 position of the glycerol backbone, while the unsaturated is in the sn2 position [56]. Therefore, the sn1-palmitoyl-sn2-oleoyl phospholipids are frequently selected for membrane models. Moreover, the PO-phospholipids have low main transition temperatures (T_m): −2 °C for POPC and 25 °C for POPE [57], which is convenient for liposome preparation. Therefore, as a model of the plasma membrane, we chose a ternary lipid mixture containing 35 % POPC, 35 % POPE, and 30 % ergosterol (mole %); we will refer to this mixture as a model fungal membrane with unsaturated lipid acyl chains (MFU). We also intended to study the effect of the saturation of the hydrophobic chains on the interactions of the model fungal membranes with cyclodiene pesticides, as often in response to environmental contamination or other shock stimuli, soil microorganisms modify the composition of their membrane phospholipids, especially the ratio of saturated and unsaturated chains [58,59]. Therefore, we constructed a second model, MFS (model fungal membrane with saturated lipid acyl chains) composed of 35 % DPPC, 35 % DPPE, and 30 % ergosterol (mole %). This model was employed only in the Langmuir monolayer studies, as due to the stiffness of the membranes and high T_m (118 °C for DPPE [57]) the formation of liposomes using this membrane composition was not feasible.

4. Preparation and studies of Langmuir monolayers

KSV NIMA double barrier Langmuir trough of the nominal area of 273 cm^2 was employed for π-A isotherms measurements. Following the standard cleaning procedure the Teflon trough was wiped with tissues soaked with chloroform, followed by a tissue soaked in isopropanol and rinsed in ultrapure water. Ultrapure MilliQ water was used in all the experiments as the subphase. Appropriate volumes of chloroform solutions of the studied substances were deposited with Hamilton analytical syringes at the air/water interface. 10 min were left for the evaporation of the spreading solvent, then the Langmuir monolayers were spread with a constant compression rate of 20 cm^2/min. Surface pressure was measured with a Wilhelmy-type electrobalance (KSV NIMA) with a rectangular plate of filtration paper (Whatman) used as a surface pressure sensor with an uncertainty of ± 0.05 mN/m. π-A isotherms were measured at least three times and the uncertainty of the mean molecular area (A) was ± 1 $Å^2$/molecule. The temperature of the subphase was controlled by a water-circulating bath. All the experiments were performed at 20 ± 0.1 °C. The compression modulus C_S^{-1} was calculated from the course of the π-A isotherms according to its definition [60]:

$$C_S^{-1} = -A\frac{d\pi}{dA} \quad (1)$$

The studied cyclodiene pesticides are not surface active and do not form Langmuir monolayers. In all the experiments performed for monolayers containing pesticides the number of film-forming lipid molecules deposited at the air/water interface was constant, regardless of the mole ratio (X) of the pesticide. All the mean molecular areas are calculated only for the lipids constituting the studied models.

Grazing incidence X-ray diffraction (GIXD) experiments were performed on the Sirius beamline of the SOLEIL synchrotron (Gif sur Yvette, France) using a dedicated surface diffractometer [61]. The description of the settings of this instrument and the performance of a routine experiment can be found in the experimental section of the reference [47]

4.1. Preparation and characterization of large unilamellar vesicles (LUV) and steady-state fluorescence anisotropy (FA) measurements

Liposome formulations were obtained from dry lipid film, prepared from the appropriate amounts (about 1 ml of the mixed solutions) of stock chloroform solutions of the studied lipids and pesticides in glass vials. The undoped LUVs were formed from POPC (35 mol%), POPE (35 mol%) and ergosterol (30 mol%). Chloroform solutions of the studied pesticides were mixed in appropriate proportion with the lipid stock solutions before the evaporation of the solvent and the formation of a dry lipid film. The original idea was to prepare liposomes with the same composition as the Langmuir monolayers, however, it was impossible to produce LUVs containing 15 or 20 mol% of CP. Thus, the CP content was lowered to effectively introduce CP into the lipid bilayer, ranging from 2.5 to 12.5 mol%. Then, the solvents were evaporated under a gentle stream of nitrogen and the samples were dried under reduced pressure. Dry lipid films were hydrated in 0.1 M PBS buffer (pH 7.4), then the vials were placed in an ultrasound bath for 1.5 h. To obtain unilamellar vesicles, the lipid suspension was subjected to five cycles of freezing (in liquid nitrogen) and thawing (60° C). Finally, the prepared mixture was extruded six times through polycarbonate filters with 100 nm pores using LiposoFast extruder (Avestin Inc.). The final concentration of lipids in each system was 1.0 mM.

The hydrodynamic diameters of the liposomes were measured with dynamic light scattering (DLS) using the Malvern Nano ZS light-scattering apparatus (Malvern Instrument Ltd., Worcestershire, UK). The sample was illuminated by the laser beam at λ = 633 nm, while the intensity of the scattered light was measured by a photodiode at the angle of 173°. Malvern software was used for the calculation of the hydrodynamic diameter and polydispersity coefficient.

The fluidity of the liposomal membrane was investigated based on the measurements of the steady-state fluorescence anisotropy (r) of DPH (1,6-diphenyl-1,3,5-hexatriene) [48]. Liposomes with this fluorescent probe were prepared by the addition of DPH solution (chloroform/methanol 4/1 v/v) to the appropriate volume of the liposomal suspensions. The final concentration of DPH in the liposomal membrane was 1.67 μM. The fluorescence anisotropy was measured with a Hitachi F-7100 spectrofluorometer. All measurements were repeated at least four times. The samples were excited with vertically polarized light at λ = 350 nm. The intensity of the emitted light was measured at λ = 428 nm both for the vertical and parallel polarization of the beam. The steady-state fluorescence anisotropy (r) was calculated using the equation:

$$r = \frac{I_{VV} - GI_{VH}}{I_{VV} - 2GI_{VH}} \quad (2)$$

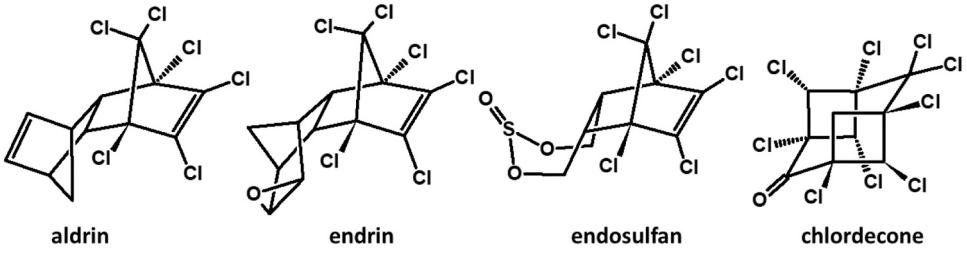

Scheme 1. Structural formulas of the studied cyclodiene pesticides.

where: $G = I_{HV}/I_{HH}$ is an instrumental correction factor which is defined as the ratio of the intensity with horizontal excitation and vertical emission to the intensity with horizontal excitation and horizontal emission, I_{VV} is the intensity with vertical excitation and vertical emission, I_{VH} is the intensity with vertical excitation and horizontal emission [48].

5. Preparation and measurements of giant unilamellar vesicles

POPC, POPE, ergosterol, and cyclodiene pesticide (ALD, END, EDS) chloroform stock solutions with concentrations of 10 mM were prepared. Appropriate volumes of the stock solutions were mixed to obtain the model membrane composition (35 % POPE, 35 % POPC, 30 % ergosterol (mole %)), or the model doped with the respective pesticide (5, 10, or 15 mol%). For FRAP (fluorescence recovery after photobleaching) experiments, the mixtures contained also 0.5 % of a fluorescent probe: 1,1'-dioctadecyl-3,3,3',3'-tetramethylindocarbocyanine perchlorate (diI C18).

GUVs were prepared by electroformation [62]. 10 μl lipid solution was spread on clean indium-tin oxide (ITO)-coated glass supports (5 μl on each glass). The ITO slides were dried for 1 h in a vacuum desiccator. Then they were assembled to sandwich a 2 mm-thick Teflon spacer, forming a formation chamber. The chamber was filled with 100 mM sucrose solution and kept at 50 °C. A sinusoidal AC electric field of the frequency of 10 Hz and field strength of 1.6 V was applied for 1 h for electroswelling of the lipid films. To ensure GUV detachment from the substrate, the frequency was lowered to 3 Hz for 5 min, and the electroformation chamber was cooled down at a rate of 1 °C/min. GUV samples were used in the experiments within 24 h of their preparation.

6. Fluorescence recovery after photobleaching (FRAP)

FRAP experiments were performed at room temperature (23±1 °C). Microscope slides were coated with casein (2 mg/ml solution). 50 μl of GUV solution was placed on the slide (22×40 mm) with a silicon spacer, covered by a coverslip (22×22 mm), and left for 1 h to allow the vesicles to sediment. The measurements were performed on a Leica TCS SP8 microscope with an HC PL FLUOTAR L 40x (0.60NA) dry objective (1 Airy unit). The samples were excited with a diode-pumped solid-state laser at 561 nm. The emission signal was collected in the 571–608 nm band with a Hyd SMD2 detector. The images (256×256 pixels) were recorded in the bidirectional scan mode at 1000 Hz. Simple Beam Expander FRAP Booster was also used. The intensity gain of the laser was set at 10 %. Three images at low laser intensity (3 %) were taken before photobleaching. Photobleaching was performed using the maximum intensity (100 %) for 268 ms (3 frames) through a circular ROI of nominal radius $r_n = 2.5$ μm. The laser was then switched back to attenuated intensity and the recovery images were recorded for several seconds. Photobleaching was performed on the upper GUV surface. The obtained data was analyzed according to a simplified equation considering molecular diffusion during photobleaching. The diffusion coefficient D was calculated according to the following equation:

$$r = \frac{I_{VV} - GI_{VH}}{I_{VV} - 2GI_{VH}} \tag{3}$$

Where: r_e and r_n are the effective and the nominal bleaching radii and $t_{1/2}$ is the half-time of fluorescence recovery. [63,64]. More information regarding the FRAP technique for the characterization of membrane fluidity can be found in references [65,66].

7. Bending rigidity

All experiments were performed at 23 °C. 50 μl of GUV solution was spread on the casein-coated glass and covered by a coverslip. Membrane fluctuations were observed using an inverted microscope (Axio Observer, Zeiss, Germany) under phase contrast using a 40x objective (NA 0.6), frame rate 20 Hz, ROI 480×480 pixels, exposure 200 ns. The number of images obtained for each GUV was 3000. The video recording and imaging were performed using a high-speed camera Pco Edge (PCO AG, Kelheim, Germany). The vesicle contours were detected and analyzed using a home-developed software that computed the bending rigidity based on the Fourier decomposition of thermally-driven membrane fluctuations into a spherical model [67,68].

8. Results and discussion

8.1. Langmuir monolayers as model fungal membranes

We first prepared single-component monolayers of the employed lipids: POPC, DPPC, POPE, DPPE, and ergosterol, measured π-A isotherms, and calculated the compression modulus. These π-A isotherms and C_S^{-1} – π curves are presented in Fig. S1 in the Supplementary Materials. Then the ternary monolayers, imitating fungal membranes, MFU, and MFS were formed and characterized. The π-A isotherms and C_S^{-1}-π dependencies for these membranes are presented in Fig. 1.

For MFU model membrane the beginning of an increase of surface pressure (lift-off area, A0) is observed at 78 Å2/mol. (Fig. 1 black curve). Upon further compression, surface pressure grows slowly, which is typical for monolayers in the liquid expanded (LE) state. At higher π values the curve is steeper and the monolayer collapses at A = 43 Å^2/mol. and π = 45 mN/m. Low values of compression modulus confirm the LE state of the MFU monolayer. For MFS A_0 = 53 Å^2/mol., π grows quickly at the compression and the curve is much steeper than measured for MFU (Fig. 1 red curve). Compression modulus exceeds the value of 100 mN/m at the molecular area of 11 Å^2/mol. and 250 mN/m at 30 Å^2/mol. achieving the maximum of 293 mN/m. These values prove high condensation of the MFS monolayer. The monolayer collapses at A = 36 Å^2/mol. and π = 50 mN/m.

The MFS model is composed of DPPC, DPPE and ergosterol. All these lipids form 2D-crystalline Langmuir monolayers when spread from chloroform solution at the air/water interface [69–71]. To check whether the lipid molecules are also periodically packed in the ternary MFS monolayer the GIXD technique was used. The GIXD data are presented in Fig. 2 and the calculated lattice parameters are collected in Table 1.

Where a, b, γ – lattice units, A_{xy} – area per one chain, τ – tilt angle of the hydrocarbon chains from the monolayer normal, L_{xy} – correlation distance within the crystalline domains.

There are three separate diffraction peaks in the I(Qxy,Qz) intensity contour map (Fig. 2a). The mutual location of these maxima is typical for an oblique 2D crystal lattice. Similar GIXD results were obtained in

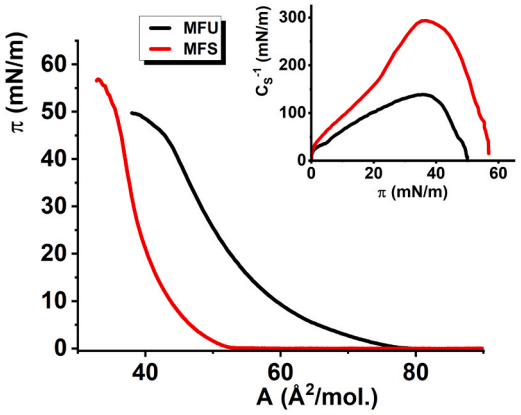

Fig. 1. Langmuir monolayer characteristic of the model fungal membranes. Surface pressure (π) – mean molecular area (A) isotherms and compression modulus (CS-1) – surface pressure (π) dependencies (inset).

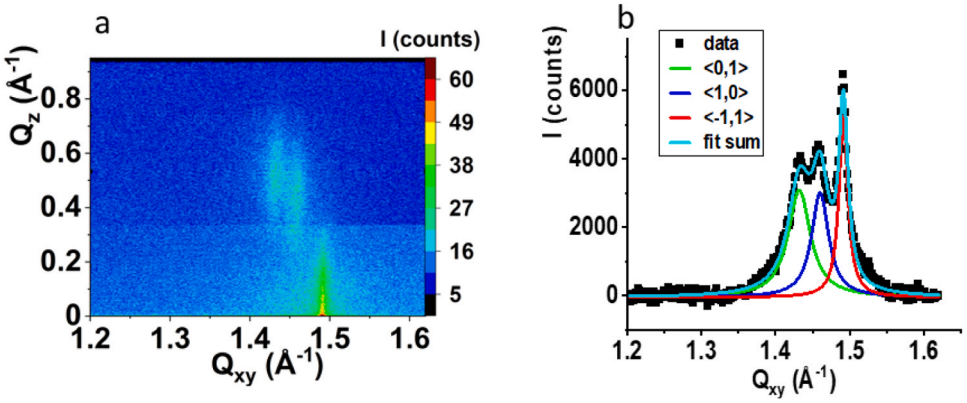

Fig. 2. Grazing incidence X-ray diffraction results for the MFS model membrane. a) I(Qxy,Qz) intensity contour map, b) I(Qxy) Bragg peak profiles. Solid lines in this plat are best fit Lorentz curves.

Table 1
Structural parameters for the MFS monolayer.

System	Q_{xy}, Q_z (Å^{-1}, Å^{-1})	Unit parameters a, b, γ (Å, Å, deg)	A_{xy} (Å^2)	τ (deg)	L_{xy} (Å)
MFS	<0,1> 1.432, 0.56 <1,0> 1.460, 0.44 <−1,1> 1.491, 0.02	4.871, 4.967, 117.9	21.37	22.3	<0,1> 149±8 <1,0> 197 ±14 <−1,1> 369±10

our previous studies in which DMPC (dimyristoyl-PC) was applied instead of DPPC (a model containing 35 % DMPC, 35 % DPPE, and 30 % ergosterol) [47]. The oblique lattice, narrow diffraction signals, and large values of L_{xy} are typical to Langmuir monolayers formed by saturated phospholipids [72], whereas for sterol monolayers, or the crystalline domains containing considerable amounts of sterol, wide non-degenerate signals with intensity maximum at ca. 1.0–1.1 Å^{-1} were typically observed [73]. The observation of narrow diffraction peaks located between 1.4 and 1.5 Å^{-1} in the reciprocal space leads to similar conclusions and interpretations to those proposed in ref. [47]. At 20 mN/m phospholipid-enriched 2D crystalline nanodomains coexist with ergosterol-rich amorphous regions. This is an important observation for further research on these systems. Since there are two phases in the system, the question arises whether pesticides will be incorporated into both of them?

8.2. *Interactions of cyclodiene pesticides with Langmuir monolayers mimicking fungal plasma membranes*

The studied cyclodiene pesticides differ significantly in their hydrophobicity. The pK_{OW} (logarithm of octanol/water partition

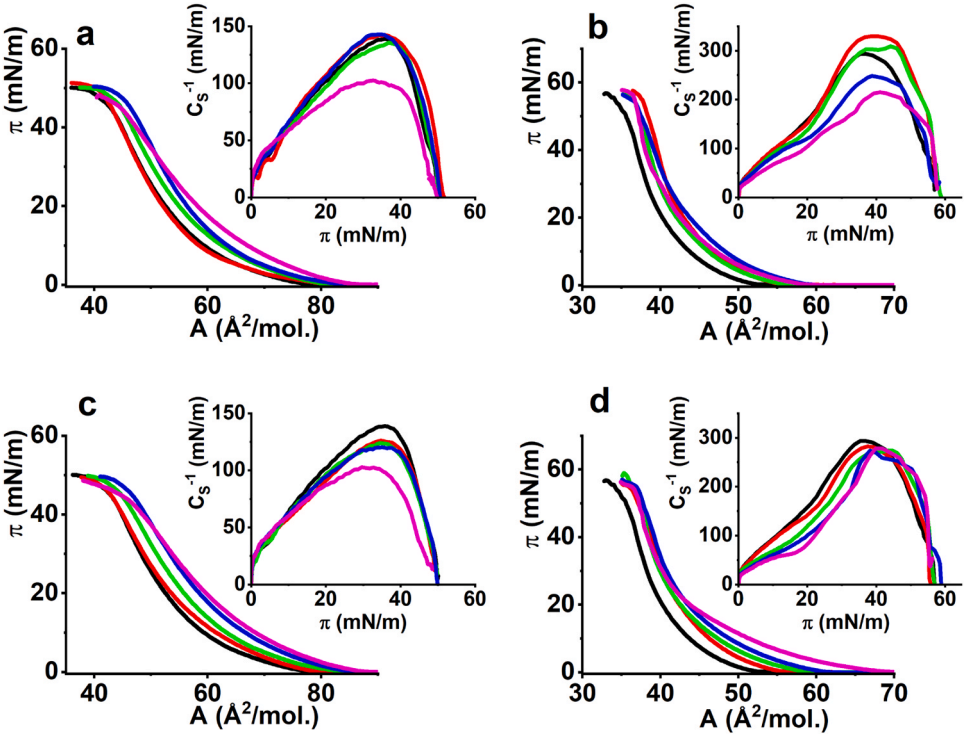

Fig. 3. Effects of aldrin and endrin presence in the model fungal membranes on their physical properties monitored by the π-A isotherms and CS-1-π dependencies. The following panels concern the systems: a) MFU + ALD, b) MFS + ALD, c) MFU + END, d) MFS + END, black – undoped membrane, red – X(CP) = 0.05, green – X (CP) = 0.10, blue – X(CP) = 0.15, magenta – X(CP) = 0.20.

coefficient) for ALD is 6.5, for END 5.2, for EDS 3.7, and for CDN 3.5 [74]. Considering the values of pK_{OW} and the fact that the scale is logarithmic it can be stated that ALD and END are much more hydrophobic than EDS and CDN. The differences in hydrophobicity of these pesticides can manifest in their membrane activity. Therefore, in further figures, the results obtained for ALD and END, and for EDS and CDN are presented separately. Fig. 3 presents the π-A isotherms and C_S^{-1} – π curves for the model membranes doped with ALD and END.

As can be seen in Fig. 3a, at X(ALD) = 0.05 the effect of the pesticide introduction into the MFU monolayer is unnoticeable, but at higher X (ALD) the π-A isotherms move successively to larger areas. It should be reminded here (see the experimental section) that the number of lipid molecules deposited at the air/water interface was constant. In such conditions a shift of the π-A isotherm toward greater molecular areas signifies a lager number of molecules present at the interface, thus the incorporation of pesticide molecules into the lipid monolayer. C_S^{-1}-π curves at X(ALD) = 0.05 – 0.15 overlap with the C_S^{-1}-π curve for the undoped MFU monolayer, which proves that the presence of ALD molecules does not affect the elasticity of the model membrane. Only at X (ALD) = 0.2, the values of C_S^{-1} are significantly lower. This may indicate the incorporation limit and the presence of ALD aggregates within the monolayer. At high surface pressure of 40 mN/m the isotherms for the monolayers doped in ALD (X(ALD) from 0.10 to 0.20) overlap, but are still shifted by 4 $Å^2$/mol. to greater mean molecular areas. The convergence of the isotherms and their further overlapping may result from the partial elimination of the incorporated ALD molecules from the model membrane. However, the 4 $Å^2$/mol. shift of these isotherms from that recorded for the undoped monolayer indicates that some ALD molecules are present in the monolayer till its collapse.

Doping the MFS model membrane with aldrin (Fig. 3b) leads to the shift of the isotherm to greater A values already at X(ALD) = 0.05, proving the incorporation of the pesticide. The increase of C_S^{-1} values indicates the condensing effect exerted on the monolayer by ALD incorporation. At the further increase of ALD content (X(ALD) from 0.10 to 0.20), the π-A isotherms are still shifted to greater A values but are located close to each other, which indicates that ALD incorporation into this model membrane is concentration limited. In the C_S^{-1}-π curves the condensing effect is still observed at X(ALD) = 0.10, while at X(ALD) = 0.15 and 0.20, the increasing number of ALD molecules leads to the decrease of compression modulus. This observation proves the postulated limited incorporation of ALD molecules into the MSF membrane. Due to this limit at X(ALD) = 0.15 and 0.20 some of the ALD molecules are separated from the lipid monolayer forming 3D aggregates, the presence of which disturbs the lipid packing within the monolayer which is reflected in the lowered C_S^{-1} values.

The addition of END into the MFU membrane (Fig. 3c) leads to an effect qualitatively and quantitatively similar to that observed when the model membrane was doped with ALD. On the other hand, significant differences between ALD and END can be observed for the model MFS composed of saturated phospholipids (Fig. 3d). With increasing X(END) a successive shift of the isotherms toward greater areas is observed. Moreover, with growing X(END) the monolayers are more expanded which manifests in lower C_S^{-1} values. This means that END molecules show greater affinity than ALD to the MFS model membrane - more pesticide molecules are incorporated and the observed changes in monolayer properties are more noticeable. However, at π > 25 mN/m, the curves approach each other, which can mean the elimination of the pesticide from the membrane.

The experiments performed using the GIXD technique for the MFS model indicated the presence of two different phases: the 2D crystalline phospholipid-rich phase, and the ergosterol-enriched amorphous, and less condensed phase. Thus, we asked a question whether ALD and END are incorporated equally into both these phases. To answer this question the MFS model membranes containing 20 mol% of ALD or END were studied with the GIXD technique. The obtained GIXD results are presented in Fig S2 and Fig. S3 of the Supplementary Materials, respectively, while the lattice parameters calculated from the GIXD data are summarized in Table S1 The CP-doped monolayers turned out to be 2D crystalline and the sequence of diffraction signals was identical within the experimental error with the results collected for the undoped MFS monolayer. Thus, the incorporation of ALD and END does not affect the crystalline packing within the model fungal membrane. As ALD and END do not affect the periodic packing of lipid molecules in the 2D crystalline nanodomains, it can be postulated that these pollutants are incorporated into the amorphous, ergosterol-rich regions of the monolayer.

The effects of the less hydrophobic CPs: EDS and CDN on the model fungal membranes were also studied and the resulting π-A isotherms and C_S^{-1}-π curves are presented in Fig. 4.

The addition of 5 mol% of EDS to the MFU model membrane shifts the π-A isotherm ca. 4 Å2/mol. to smaller A values (Fig. 4a). This shift with a slight increase in compression modulus proves the condensing effect exerted by EDS on the MFU monolayer. EDS molecules, unlike ALD and END, have a permanent dipole moment, have a permanent dipole moment, thanks to which they can interact with the polar headgroups of phospholipid molecules. It can be assumed that EDS molecules are located in the monolayer between the initial part of the hydrocarbon chains of phospholipid molecules so that their more strongly hydrated hydroxide fragment comes into contact with the polar headgroup. This leads to a more compact monolayer packing manifesting in increased CS-1 values. The overlapping of the π-A isotherms for the monolayer at X(EDS) = 0.10 and the undoped membrane also seems to originate from this effect. At higher EDS contents, the isotherms are shifted toward greater A values, to the right of the isotherm registered for the MFU monolayer. More significant effects of the presence of EDS are observed for the MFS model membrane (Fig. 4b). At X(EDS) = 0.05, the lift-off area A0 is reduced from 53 Å2/mol. (undoped MFS) to 43 Å2/mol. This strong condensing effect finds its manifestation in the significant increase in CS-1 values. At X(EDS) = 0.10 A0 = 48 Å2/mol., which is still 5 Å2/mol. smaller than for the undoped monolayer. At lower π the isotherm is shifted to lower A values, but starting from 15 mN/m practically overlaps with the isotherm measured for the undoped MFS monolayer. The CS-1 – π curve overlaps with the curve for X(EDS) = 0.05, thus, also in this case a significant condensing effect was observed. For X(EDS) = 0.15 A0 was 61 Å2/mol., and for X(EDS) = 0.2 67.5 Å2/mol., that is 8 and 14.5 Å2/mol. greater than noticed for the undoped MFS monolayer. At π = 30 mN/m the isotherms for X(EDS) = 0.15 and 0.20 overlap, which indicates possible elimination of EDS molecules from the monolayer. At X(EDS) = 0.15 and 0.20 CS-1 values are lower than for the undoped monolayer, thus, when the content of EDS in the membrane environment is too high the trend reverts and the molecules of this pesticide expand the model membrane.

CDN addition to the MFU monolayer causes a significant increase in compression modulus (Fig. 4c). This observation first indicates the effective incorporation of CDN molecules into the membrane. Similar to EDS, CDN molecules also possess a permanent dipole moment and interact with the headgroups of phospholipid molecules forcing them to be pecked more closely. Despite the observed condensing effect the π-A isotherms for X(CDN) = 0.05 and 0.10 are shifted to higher A values, which originates from the bulky structure of the CDN molecule. The shift at collapse is 6 Å2/mol., which proves that even at high surface pressures some CDN molecules remain incorporated into the MFU monolayer. At higher CDN contents, X(CDN) = 0.15 and 0.20 the isotherms shift progressively to greater A values. At X(CDN) = 0.15 the increase of CS-1 value is still observed, while at X(CDN) = 0.2, CS-1 values are noticeably lower. This decrease in compression modulus may be caused by the limited incorporation of this pesticide and the formation of 3D aggregates by the excess CDN molecules. The effects exerted by the incorporation of CDN molecules into the MFS membrane are even more pronounced (Fig. 4d). The isotherms shift progressively to greater mean molecular areas with increasing X(CDN). At X(CDN) = 0.2 A0 = 69 Å2/mol., so is 16 Å2/mol. greater than for the undoped monolayer. Only for

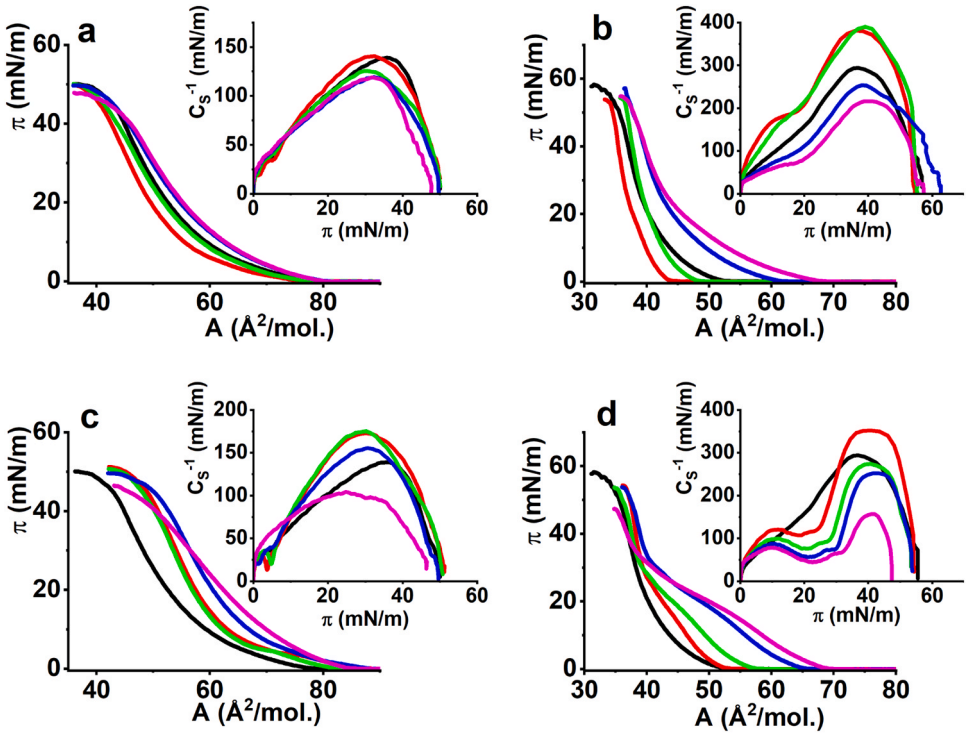

Fig. 4. Effects of endosulfan and chlordecone presence in the model fungal membranes on their physical properties monitored by the π-A isotherms and CS-1-π dependencies. The following panels concern the systems: a) MFU + EDS, b) MFS + EDS, c) MFU + CDN, d) MFS + CDN, black – undoped membrane, red – X(CP) = 0.05, green – X(CP) = 0.10, blue – X(CP) = 0.15, magenta – X(CP) = 0.20.

X(CDN) = 0.05 the increased condensation of the doped monolayer was observed, for higher X(CDN) CS-1 values are lower than for the undoped membrane. A shallow minimum observed in the course of the CS-1- π curves between 20 and 30 mN/m indicates a phase transition in the model membrane, which can originate from the progressive separation of CDN molecules from the monolayer.

The MFS model membranes containing 20 mol% of EDS or CDN were studied with the GIXD technique. The obtained GIXD results are presented in Fig S4 and Fig. S5 of the Supplementary Materials, respectively, while the lattice parameters calculated from the GIXD data are summarized in Table S2. Again, just like for ALD and END, the diffractograms recorded for the EDS and CDN-doped monolayers are identical within the limit of experimental error with the diffractogram measured for the undoped MFS model membrane. This leads to the same interpretation, in which we suggest the incorporation of the cyclodiene pesticide molecules into the ergosterol-enriched amorphous phase in the MFS monolayers

Mycoremediation is an effective remediation strategy for cyclodiene pesticide-contaminated soils [34,75–78]. However, mycoremediation as an option of bioaugmentation is frequently ineffective. The reasons can be different, however, the antifungal toxicity of POPs plays here an important role. In our contribution we postulated the membrane-destructive activity of cyclodiene pesticides as a possible explanation for this situation. However, the incorporation of a hydrophobic pollutant into a plasma membrane is not equivalent to membrane destructive activity. Multiple metabolic transformations of hydrophobic pollutants take place in the membranes, so some membrane accumulation of a given pollutant is necessary in the biodegradation process [79]. The optimal option is a situation in which the accumulation of pollutant molecules in the membrane minimally affects its physical properties and self-organization. Our results discussed so far indicate that all four investigated cyclodiene pesticides can be incorporated into both used by us fungal membrane models. The limit mole proportion for the pesticide incorporation is around 0.15. For higher mole proportion the excess pesticide molecules separate from the lipid matrix forming probably multilayer aggregates. The pesticide incorporation affected the MFS model more than MFU, so to high proportion of saturated membrane lipids is unfavorable in mycoremediation. The studies performed on four cyclodiene pesticides most commonly found as soil contaminants prove also that CDN is not less membrane active than the other three cyclodiene pesticides much earlier listed in the Anex A of Stockholm Convention. CDN was applied mainly in tropical countries in banana plantations against banana weevil. Its vast application has led to heavy and persistent contamination. Based on a model elaborated by Cabidoche and co-authors, it can be predicted that CDN-caused contamination of tropical soils can last decades or even hundreds of years, depending on the organic matter content in the soils [80]. Bioremediation is the only cure for these soils. However, this pesticide is very toxic to soil microorganisms, reduces their biodiversity and only a few of them can biodegrade this pesticide. Merlin and co-authors [81] studied the CDN biodegradation potential of 11 genera of soil fungi, and it turned out that only one isolate, Fusarium oxysporum MIAE01197 was able to grow in CDN-polluted soil and biodegrade this pesticide. The fungal toxicity of CDN is probably related to the membrane-destructive activity of this pesticide. CDN, C10Cl10O is closely related to mirex C10Cl12. Both compounds differ at one carbon atom – the -CCl2- group is exchanged in CDN to ketone -C═O. This structural change lowers the value of pKOW from 6.9 for mirex to 3.5 for CDN [74] and significantly increases the membrane activity of the pesticide. In our previous studies, we found out, that mirex incorporation to phospholipid Langmuir monolayers is very limited [82]. This compound did not build into the phospholipid matrix, but formed multiple 3D aggregates; therefore, we expected a similar behavior for CDN. However, our studies proved, that CDN behaves completely differently. Although it is similarly bulky as mirex and structurally incompatible with hydrocarbon chains, it is easily incorporated into the model membrane. The perchlorinated symmetrically substituted mirex molecule is completely non-polar, whereas the introduction of the ketone group induces the permanent dipole moment in this molecule. The dipolar properties of CDN are responsible for the drastic change in pKOW observed for this compound. The dipolar

properties of CDN and also EDS as compared with ALD and END, facilitate the interactions of these CP molecules with the polar head-groups of membrane phospholipids, which can stabilize these molecules in the membrane.

The studies performed on Langmuir monolayers shed light on the differences in membrane activity of the studied CPs and indicate, which of them can be more easily incorporated into the plasma membrane. However, the studies do not conclude on the effects exerted by the incorporated CP molecules on membrane fluidity and stiffness. Therefore, we employed LUV and GUV liposomes as alternative membrane models to study these phenomena.

Application of LUV and GUV liposomes in the studies of CP–model fungal membrane interactions

The DI-X(CP) and φ-X(CP) dependencies are presented in Fig. S6 of the Supplementary Materials. The obtained LUVs were highly monodisperse, with a DI coefficient ranging from 0.08 to 0.1. The hydrodynamic diameters of the liposomes φ ranged from 100 to 130 nm. For LUV enriched in the DPH fluorescent probe steady-state fluorescence anisotropy (FA) measurements were performed. The resulting plots are shown in Fig. 5.

With increasing content of the CP molecules in the membrane environment, the anisotropy of DPH falls to the limiting value of ca. 0.09 – 0.095 (Fig. 5). The observed trend indicates that the presence of all the studied CP molecules increases the membrane fluidity and that the effect is concentration-dependent. These observations partly diverge from those obtained for Langmuir monolayers. The studies conducted on Langmuir monolayers showed a condensing effect of chlordecone on the elasticity of the MFU membrane. It should be highlighted, that both membrane models are complementary but have different physical parameters. The envelope of a liposome is a bilayer, so the thickness of the hydrocarbon chain region is doubled compared with a monolayer. CP molecules prefer a hydrophobic environment, so they can more effectively avoid contact with water and water-hydrated polar headgroups when located in a bilayer. The use of Langmuir monolayers reveals the differences between the tested molecules related to their hydrophobicity. CDN, possessing a considerable dipole moment, interacts strongly with the polar headgroups, and by this induces reorientations of the hydrocarbon chains leading to the increase of monolayer condensation. In LUVs, all the tested CP molecules are isolated from the lipid headgroups, which eliminates the differences between them. All the tested CPs affect the fluidity of the model membrane, which may be important for the mechanism of CP fungal toxicity.

To verify the observations made for LUVs, studies on GUV liposomes were performed. Only the structurally similar CP molecules: ALD, END, and EDS were tested. Fig. 6 shows the diffusion coefficients (D) obtained using the FRAP technique.

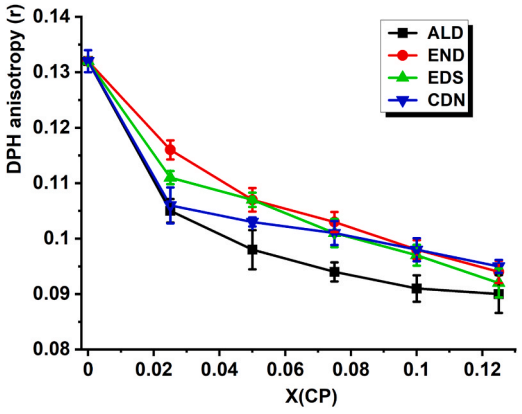

Fig. 5. Effects of cyclodiene pesticides on bilayer fluidity monitored by fluorescence anisotropy. Dependence of DPH anisotropy, r, on the content of the studied CP in the lipid bilayer.

Both fluorescence anisotropy and FRAP probe the fluidity of the model membranes, however, while the former monitors the rotation of the rod-like DPH molecule in the hydrophobic membrane environment, FRAP reports the translational migration of a fluorescent probe in the monolayer plane [63]. FRAP provides additional insight into monolayer fluidity, but the experiment using this technique must be performed on a sufficiently large object that can be imaged using optical microscopy. Therefore, thanks to the use of GUV liposomes, it was possible to perform these experiments and make sure whether the conclusions drawn from LUV measurements were correct. The calculated values of D agree with the data accessible for similar lipid systems [62,83,84]. For X (ALD) = 0.05 a rise of the mean D value from 10 to 12 μm2/s is observed, meaning that the small addition of this pesticide increases the fluidity of the model membrane (Fig. 6). However, at higher X(ALD) of 0.10 and 0.15 D values are practically identical to those observed for the undoped membrane. For END D rises with the pesticide content approximately linearly from X(END) = 0 to X(END) = 0.10, whereas the value for X(END) = 0.15 is lower than at X(END) = 0.10, which distorts this trend. For EDS, the diffusion coefficient rises monotonically with increasing X(EDS) achieving the value of 13 μm2/s for X(EDS) = 0.15. It can be stated that for END and EDS the results obtained for LUV (fluorescence anisotropy) and here for GUV agree, at least till X(pesticide) = 0.10. The introduction of these CP into the model membrane leads to its fluidization, progressing with the increasing content of these pesticides. The discrepancies observed for ALD can be concentration-dependent. Aldrin mole proportions applied in the LUV studies were lower than in the experiments performed on GUVs. For X(ALD) = 0.05 the results are convergent but for X(ALD) = 0.10 and 0.15, the results diverge, which can be connected with the limited incorporation of ALD into the model bilayer membranes. On the other hand, these results are in full agreement with those obtained in the studies performed on Langmuir monolayers. At X(ALD) = 0.10 and 0.15, the incorporation of ALD into the model membrane did not affect its condensation, whereas the incorporation of END and EDS led to the expansion of the monolayer.

Another membrane parameter that we explored to probe the effect of CP incorporation into the GUVs was the membrane bending rigidity κ. The dependence of this parameter on X(CP) is illustrated in Fig. 7.

The bending rigidity reflects how flexible the membrane is [85]. The CP-free membrane exhibits bending rigidity values close to that of pure POPC membranes. The insertion of aldrin and endrin increases the membrane stiffness, while the less hydrophobic EDS molecule does not affect the stiffness of the model membrane. Also here, the highest concentration, X(CP) = 0.15, clearly deviates from the observed trend, as the values are lower than at X(CP) = 0.10. This finding might signify limited CP incorporation into the bilayer, or more probably, possible aggregation of the pesticide molecules within the bilayer, sequestering a large fraction of them with some of the lipids and depleting the remaining bilayer of the pesticide. The increased stiffness of the membrane caused by ALD and END incorporation can impair its proper functioning.

9. Conclusions

Soil contamination with polychlorinated pesticides is a serious problem, especially in tropical countries, where these pesticides have been used until recently or even still are being introduced into the environment despite bans. Depending on the conditions in the soil, the half-life coefficients of these pesticides can be up to several decades. Mycoremediation, which involves the introduction of appropriate strains of fungi into contaminated soils can be an effective option for accelerating the degradation of soil-accumulated CPs. However, CPs exhibit fungicidal activity, which can lead to the death of the fungal cells introduced into the contaminated soil. The significant hydrophobicity of CP molecules may cause their accumulation in fungal plasma membranes leading to their disfunctions. In our studies, we used both monolayer and multilayer models of fungal membranes to better

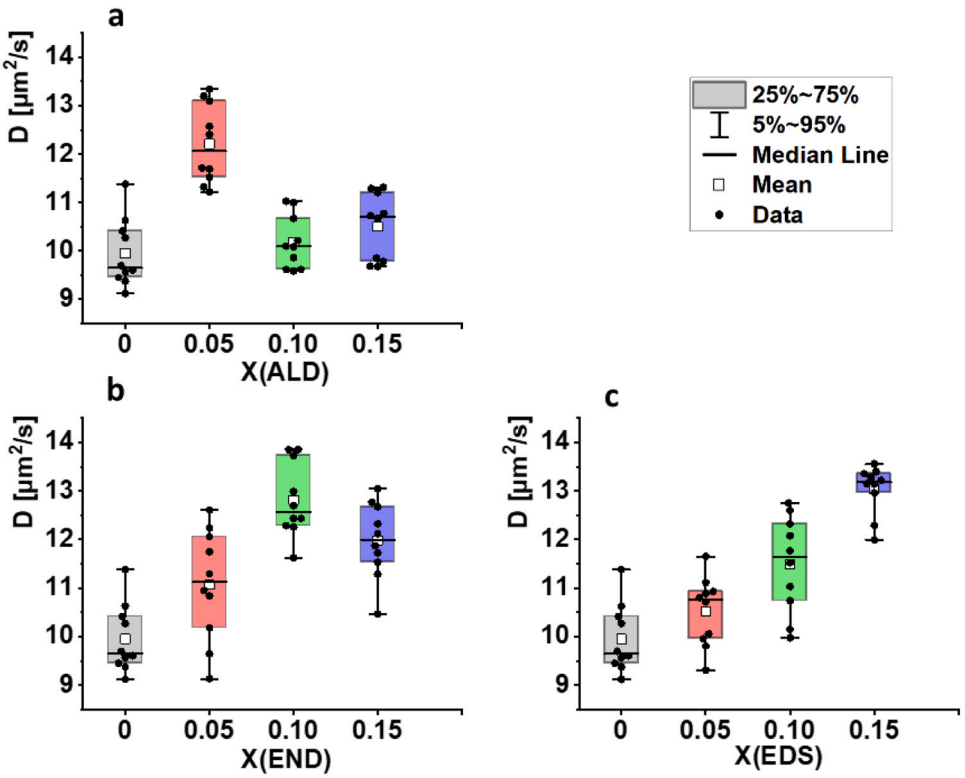

Fig. 6. Fluorescence recovery after photobleaching (FRAP) results for GUV liposomes (of the MFU composition) doped with a) ALD, b) END, and c) EDS. The data presents the diffusion coefficients of diIC18 fluorescent probe.

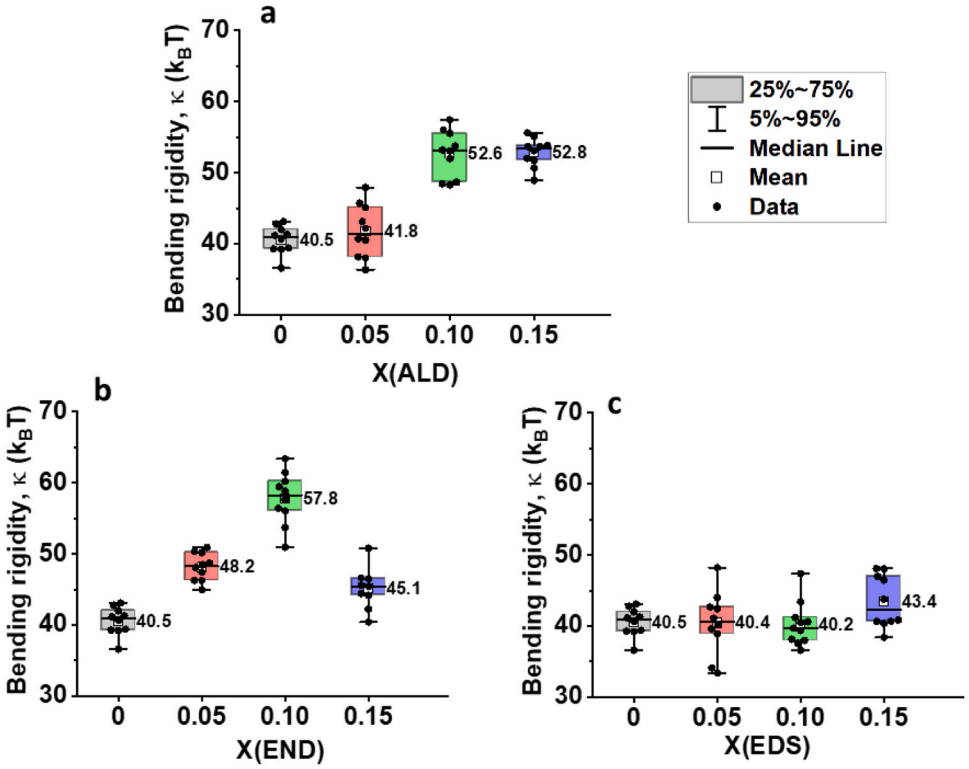

Fig. 7. Effect of the incorporation of CP pesticides on the membrane bending rigidity assessed from an analysis of the thermal fluctuations of GUVs doped in:: a) ALD, b) END, c) EDS.

understand the interactions of CP molecules with membrane lipids. Our studies have shown that all CPs we tested can be incorporated into model membranes up to a molar ratio of approximately 0.15. Regarding Langmuir monolayers, the more polar CPs as endosulfan and especially chlordecone had a stronger impact on the physical properties of these model membranes. GIXD experiments proved that in the MSF model formed of saturated phospholipids two different phases coexist – a 2D crystalline phospholipid-rich phase and an amorphous ergosterol enriched phase. CPs are incorporated into the amorphous phase and their presence do not disturb the formation of the crystalline nano-domains. This is an important observation, as it can be assumed that in real membranes accumulated CPs will not hinder the formation of highly organized self-assembled domains, such as for example lipid rafts. The experiments performed on liposomes have proven that the incorporation of all the studied CP molecules into the bilayer leads to its fluidization. Moreover, the bending rigidity studies indicated that aldrin and endrin, that is the more hydrophobic CPs, can limit the conformational freedom of phospholipid hydrocarbon chains and lead to local stiffening of the bilayer. However, all these effects were not drastic, which predisposes fungal cells to be used in the remediation of soils contaminated with polychlorinated cyclodiene pesticides.

CRediT authorship contribution statement

Marzena Mach: Investigation. **Rumiana Dimova:** Validation, Supervision, Conceptualization. **Vasil N. Georgiev:** Investigation. **Mareike S. Stephan:** Investigation. **Aneta Wójcik:** Investigation. **Marcin Broniatowski:** Writing – original draft, Supervision, Methodology, Investigation, Funding acquisition, Formal analysis, Data curation, Conceptualization. **Paweł Wydro:** Investigation.

Declaration of Competing Interest

The authors declare that they have no known competing financial interests or personal relationships that could have appeared to influence the work reported in this paper.

Data availability

Data will be made available on request.

Acknowledgements

This project was financed by the National Science Centre (No 2016/21/B/ST5/00245). We gratefully acknowledge SOLEIL for the provision of synchrotron radiation facilities and we would like to thank Dr. Philippe Fontaine for assistance in using SIRIUS beamline. M.S. acknowledges funding from the International Max Planck Research School on Multiscale Biosystems.

Appendix A. Supporting information

Supplementary data associated with this article can be found in the online version at doi:10.1016/j.colsurfa.2024.134970.

References

[1] T.G. Ambaye, A. Hossani, M. Vaccari, A. Franzetti, S. Prasad, F. Formicola, A. Rosatelli, M.Z. ur Rehman, G. Mohanakrishna, S.V. Ganachari, T. M. Aminabhavi, S. Rtimi, Emerging technologies for the removal of pesticides from contaminated soils and their reuse in agriculture, Chemisphere 362 (2024) 142433, https://doi.org/10.1016/j.chemosphere.2024.142433.

[2] B. Beig, M.B.K. Niazi, F. Sher, Z. Jahan, M. Zia, G.A. Shah, A.A. Ghfar, Z. Iqbal, Development and testing of environment friendly nanohybrid coatings for sustainable agriculture technologies, Environ. Res. 240 (2024) 117546, https://doi.org/10.1016/j.envres.2023.117546.

[3] N.El. Houda Boughattas, F. Katlane, R. Amami, S.C. Kefauver, K. Abrougui, M. S. Naceur, M. Hameed, H. Ghazouani, Z. Hussain, S. Ansar, F. Sher, Improving estimation of water soil erosion by introducing lithological formation for environmental remediation, Environ. Res. 231 (2023) 116210, https://doi.org/10.1016/j.envres.2023.116210.

[4] R. Ying, W. Gang, B. Xuanjiao, S. Yuying, Z. Zheng, H. Jianping, Research progress on remediation of organochlorine pesticide contamination in soil, Environ. Geochem. Health 46 (2024) 25, https://doi.org/10.1007/s10653-023-01797-0.

[5] B. Yuan, S. Zhang, D. Ren, X. Zhang, Research progress on the removal of heavy metals in water and soil by modified carbon nanotubes: a review, Water Air Soil Pollut. 235 (2024) 418, https://doi.org/10.1007/s11270-024-07238-7.

[6] T. Rasheed, S. Shafi, F. Sher, Smart nano-architectures as potential sensing tools for detecting heavy metal ions in aqueous matrices, Trends Environ. Anal. Chem. 36 (2022) e00179, https://doi.org/10.1016/j.teac.2022.e00179.

[7] Y. Hu, J. Wang, Y. Yang, S. Li, Q. Wu, E. Nepovimova, X. Zhang, K. Kuca, Revolutionizing soil heavy metal remediation: Cutting-edge innovations in plant disposal technology, Sci. Total Environ. 918 (2024) 170577, https://doi.org/10.1016/j.scitotenv.2024.170577.

[8] M. Zhang, Q. Chen, Z. Gong, Microbial remediation of petroleum-contaminated soil focused on the mechanism and microbial response: a review, Environ. Sci. Pollut. Res. 31 (2024) 33325–33346, https://doi.org/10.1007/s11356-024-33474-9.

[9] Stockholm Convention, www.pops.int.

[10] L.P. Padhye, P. Srivastava, T. Jasemizad, S. Bolan, D. Hou, S.M. Shaheen, J. Rinklebe, D. O'Connor, D. Lamb, H. Wang, K.H.M. Siddique, N. Bolan, Contaminant containment for sustainable remediation of persistent contaminants in soil and groundwater, J. Hazard. Mat. 455 (2023) 131575, https://doi.org/10.1016/j.jhazmat.2023.131575.

[11] S. Bolan, L.P. Padhye, C.N. Mulligan, E. Ritore-Alonso, R. Saint-Fort, T. Jasemizad, C. Wang, T. Zhang, J. Rinklebe, H. Wang, K.H.M. Siddique, M.B. Kirkham, N. Bolan, Surfactant-enhanced mobilization ofpersistent organic pollutants: potential for soil and sediment remediation and unintended consequences, J. Hazard. Mater. 443 (2023) 130189, https://doi.org/10.1016/j.jhazmat.2022.130189.

[12] D. Rosner, G. Markowitz, Persistent pollutants: a brief history of the discovery of the widespread toxicity of chlorinated hydrocarbons, Environ. Res. 120 (2013) 126–133, https://doi.org/10.1016/j.envres.2012.08.011.

[13] R. Jayarai, P. Megha, P. Sreedev, Organochlorine pesticides, their toxic effects on living organisms and their fate in the environment, Interdiscip. Toxicol. 9 (2016) 90–100, https://doi.org/10.1515/intox-2016-0012.

[14] Y. Luan, Z. Ye, Y. Zhang, R. Hu, X. Hu, L. Wei, Y. Guo, Y. Fang, Hexachloropentadiene in soil, air, and biota around an agrochemical factory: concentrations, distribution, and risk evaluation, Arch. Environ. Contam. Toxicol. 83 (2022) 242–252, https://doi.org/10.1007/s00244-022-00957-0.

[15] R. Carson, Silent Spring; Houghton Mifflin Company: Boston, MA, 1962.

[16] M. Ali, A.A. Kazmi, N. Ahmed, Study on effects of temperature, moisture, and pH in degradation and degradation kinetics of aldrin, endosulfan, lindane pesticides during full-scale continuous rotary drum composting, Chemosphere 102 (2014) 68–75, https://doi.org/10.1016/j.chemosphere.2013.12.022.

[17] A. Buah-Kwofie, M.S. Humphries, Validation of a modified QuEChERS method for the analysis of organochlorine pesticides in fatty biological tissues using two-dimensional gas chromatography, J. Chromatogr. B 1105 (2019) 85–92, https://doi.org/10.1016/j.jchromb.2018.12.010.

[18] J. Abraham, S. Silambarasan, Biomineralization and formulation of endosulfan degrading bacterial and fungal consortiums, Pestic. Biochem. Physiol. 116 (2014) 24–31, https://doi.org/10.1016/j.pestbp.2014.09.006.

[19] P.L. Saaidi, O. Grünberger, A. Samouëlian, Y. Le Roux, A. Richard, D.A. Devault, C. Feidt, P. Benoit, O. Evrard, G. Imfeld, C. Mouvet, M. Voltz, Is dissipation half-life of 5 years for chlordecone in soils of French West Indies relevant? Environ. Pollut. 324 (2023) 121283 https://doi.org/10.1016/j.envpol.2023.121283.

[20] S.N. Khuman, M.K. Park, H.J. Kim, S.M. Hwang, C.H. Lee, S.D. Choi, Organochlorine pesticides in the urban, suburban, agricultural, and industrial soil in South Korea after three decades of ban: Spatial distribution, sources, time trend, and implicated risks, Environ. Pollut. 311 (2022) 119938, https://doi.org/10.1016/j.envpol.2022.119938.

[21] S.N. Khuman, P.G. Vinod, G. Bharat, Y.S.M. Kumar, P. Chakraborty, Spatial distribution and compositional profiles of organochlorine pesticides in the surface soil from the agricultural, coastal and backwater transects along the South-west coast of India, Chemosphere 254 (2020) 126699, https://doi.org/10.1016/j.chemosphere.2020.126699.

[22] H. Harms, D. Schlosser, L.Y. Wick, Untapped potential: exploiting fungi in bioremediation of hazardous chemicals, Nat. Rev. Microbiol. 9 (2011) 177–192, https://doi.org/10.1038/nrmicro2519.

[23] Z. Maqbool, S. Hussain, M. Imran, F. Mahmood, T. Shahzad, Z. Ahmed, F. Azeem, S. Muzammil, Perspectives of using fungi as bioresource for bioremediation of pesticides in the environment: a critical review, Environ. Sci. Pollut. Rev. 23 (2016) 16904–16925, https://doi.org/10.1007/s11356-016-7003-8.

[24] A. D'Annibale, F. Rosetto, V. Leonardi, F. Federici, M. Petruccioli, Role of autochthonous filamentous fungi in bioremediation of a soil historically contaminated with aromatic hydrocarbons, Appl. Environ. Microbiol. 72 (2006) 28–36, https://doi.org/10.1128/AEM.72.1.28-36.2006.

[25] G.R. Tortella, M.C. Diez, N. Duran, Fungal diversity and use in decomposition of environmental pollutants, Crit. Rev. Microbiol. 31 (2005) 197–212, https://doi.org/10.1080/10408410500304066.

[26] E. Marco-Urrea, L. Garcia-Romera, E. Aranda, Potential of non-ligninolytic fungi in bioremediation of chlorinated and polycyclic aromatic hydrocarbons, N. Biotechnol. 32 (2015) 620–628, https://doi.org/10.1016/j.nbt.2015.01.005.

[27] G. Zafra, A.E. Absalón, D.V. Cortés-Espinosa, Morphological changes and growth of filamentous fungi in the presence of high concentrations of PAHs, Braz. J.

Microbiol. 46 (2015) 937–941, https://doi.org/10.1590/S1517-838246320140575.
[28] R.A. Videira, M.C. Antunes-Madeira, V.M.C. Madeira, Perturbations induced by α- and β-endosulfan in lipid membranes: a DSC and fluorescence polarization study, Biochim. Biophys. Acta 1419 (1999) 155–163, https://doi.org/10.1016/S0005-2736(99)00060-7.
[29] M.C. Antunes-Madeira, V.M.C. Madeira, Membrane fluidity as affected by the insecticide lindane, Biochim. Biophys. Acta 982 (1989) 161–166, https://doi.org/10.1016/0005-2736(89)90187-9.
[30] R.T. Kapoor, J. Zdarta, Fabrication of engineered biochar for remediation of toxic contaminants in soil matrices and soil valorization, Chemosphere 358 (2024) 142101, https://doi.org/10.1016/j.chemosphere.2024.142101.
[31] U. Khalid, F. Sher, S. Noreen, E.C. Lima, T. Rasheed, S. Sehar, R. Amami, Comparative effects of conventional and nano-enabled fertilizers on morphological and physiological attributes of Caesalpinia bonducella plants, J. Saudi Soc. Agric. Sci. 21 (2022) 61–72, https://doi.org/10.1016/j.jssas.2021.06.011.
[32] I. Ziani, A. El Guerraf, N.E. Bentouhamie, M. Brahmi, H. Bouakline, A. El Bachiri, M.L. Fauconnier, S. Ansar, F. Sher, Nanoreinforcement strategies for enhancing biodegradable composites in biochemical applications within agriwaste valorisation, Biocatal. Agric. Biotechnol. 58 (2024) 103223, https://doi.org/10.1016/j.bcab.2024.103223.
[33] R.A. Simmer, J.L. Schnoor, Phytoremediation, bioaugmentation, and the plant microbiome, Environ. Sci. Technol. 56 (2022) 16602–16610, https://doi.org/10.1021/acs.est.2c05970.
[34] P. Bokade, H.J. Purohit, A. Bajaj, Myco-remediation of chlorinated pesticides: Insights into fungal metabolic system, Indian J. Microbiol. 61 (2021) 237–249, https://doi.org/10.1007/s12088-021-00940-8.
[35] C.E. Cerniglia, Fungal metabolism of polycyclic aromatic hydrocarbons: past, present and future applications in bioremediation, J. Ind. Microbiol. Biotechnol. 19 (1997) 324–333, https://doi.org/10.1038/sj.jim.2900459.
[36] R. Kataoka, Biodegradability and biodegradation pathways of chlorinated cyclodiene insecticides by soil fungi, J. Pestic. Sci. 43 (2018) 314–320, https://doi.org/10.1584/jpestics.J18-03.
[37] A. Kaewlaoyoong, C.Y. Cheng, C. Lin, J.R. Chen, W.Y. Huang, P. Sriprom, White rot fungus Pleurotus pulmonarius enhanced bioremediation of highly PCDD/F-contaminated field soil via solid state fermentation, Sci. Total. Environ. 738 (2020) 139670, https://doi.org/10.1016/j.scitotenv.2020.139670.
[38] R.K. Rajendran, C.C. Lin, S.L. Huang, R. Kirschner, Enrichment, isolation, and biodegradation potential of long-branched chain alkylphenol degrading non-ligninolytic fungi from wastewater, Mar. Pollut. Bull. 125 (2017) 416–425, https://doi.org/10.1016/j.marpolbul.2017.09.042.
[39] T.S. Bhalerao, P.R. Puranik, Biodegradation of organochlorine pesticide, endosulfan, by a fungal soil isolate. Aspergillus niger, Int. Biodeter. Biodeg. 59 (2007) 315–321, https://doi.org/10.1016/j.ibiod.2006.09.002.
[40] K.S. Ahmad, Remedial potential of bacterial and fungal strains (Bacillus subtilis, Aspergillus niger, Aspergillus flavus and Penicillium chrysogenum) against organochlorine insecticide endosulfan, Folia Microbiol 65 (2020) 801–810, https://doi.org/10.1007/s12223-020-00792-7.
[41] J.A. Salam, N. Das, Lindane degradation by candida VITJzN04, a newly isolated yeast strain from contaminated soil: Kinetic study, enzyme analysis and biodegradation pathway, World J. Microbiol. Biotechnol. 30 (2014) 1301–1313, https://doi.org/10.1007/s11274-013-1551-6.
[42] T. Janicki, M. Krupiński, J. Długoński, Degradation and toxicity reduction of the endocrine disruptors nonylphenol, 4-tert-octylphenol and 4-cumylphenol by the nonligninolytic fungus Umbelopsis isabelline, Biores. Technol. 200 (2016) 223–229, https://doi.org/10.1016/j.biortech.2015.10.034.
[43] A. Ceci, L. Pierro, C. Riccardi, F. Pinzari, O. Maggi, A.M. Persiani, G.M. Gadd, M. P. Papini, Biotransformation of β-hexachlorocyclohexane by the saprotrophic soil fungus Penicillium griseofulvum, Chemosphere 137 (2015) 101–107, https://doi.org/10.1016/j.chemosphere.2015.05.074.
[44] M. Bhatt, T. Cajthami, V. Sasek, Mycoremediation of PAH-contaminated soil, Folia Microbiol 47 (2002) 255–258, https://doi.org/10.1007/BF02817647.
[45] O. Potin, C. Rafin, E. Veignie, Bioremediation of an aged polycyclic aromatic hydrocarbons (PAHs)-contaminated soil by filamentous fungi isolated from the soil, Int. Biodeter. Biodeg. 4154 (2004) 45–52, https://doi.org/10.1016/j.ibiod.2004.01.003.
[46] M.C. Medaura, M. Guivernau, X. Moreno-Ventas, F.X. Prenafeta-Boldú, M. Viñas, Bioaugmentation of native fungi, an efficient strategy for the bioremediation of an aged industrially polluted soil with heavy hydrocarbons, Front. Microbiol. 12 (2021) 626436, https://doi.org/10.3389/fmicb.2021.626436.
[47] A. Wójcik, M. Stephan, W. Ryczek, K. Olechowska, P. Wydro, R. Dimova, M. Broniatowski, Interactions of polycyclic aromatic hydrocarbons and their nitro derivatives with bilayer and monolayer models of fungal membranes, J. Mol. Liq. 360 (2022) 119591, https://doi.org/10.1016/j.molliq.2022.119591.
[48] P. Perczyk, M. Młyńczak, P. Wydro, M. Broniatowski, Persistent organic pollutants in model fungal membranes. Effects on the activity of phospholipases, Biochim. Biophys. Acta 1864 (2022) 184018, https://doi.org/10.1016/j.bbamem.2022.184018.
[49] P.J. Brennan, D.M. Losel, Physiology of fungal lipids: selected topics, Adv. Microb. Physiol. 17 (1978) 47–179, https://doi.org/10.1016/s0065-2911(08)60057-0.
[50] P. Bernat, J. Nykiel-Szymańska, P. Stolarek, M. Słaba, R. Szewczyk, S. Różalska, 2,4-dichlorophenoxyacetic acid-induced oxidative stress: metabolome and membrane modifications in Umbelopsis isabellina, a herbicide degrader, PLoS ONE 13 (2018) e0199677, https://doi.org/10.1371/journal.pone.0199677.
[51] A.I.P.M. de Kroon, P.J. Rijken, C.H. de Smet, Checks and balances in membrane phospholipid class and acyl chain homeostasis, the yeast perspective, Prog. Lipid Res. 4752 (2013) 374–394, https://doi.org/10.1016/j.plipres.2013.04.006.
[52] P. Perczyk, A. Wójcik, P. Wydro, M. Broniatowski, The role of phospholipid composition and ergosterol presence in the adaptation of fungal membranes to harsh environmental conditions – membrane modeling study, Biochim. Biophys. Acta 1862 (2020) 183136, https://doi.org/10.1016/j.bbamem.2019.183136.
[53] J. Loffler, H. Einsele, H. Hebart, U. Schumacher, C. Hrastnik, G. Daum, Phospholipid and sterol analysis of plasma membranes of azole-resistant Candida albicans strains, FEMS Microbiol. Lett. 185 (2000) 59–63, https://doi.org/10.1111/j.1574-6968.2000.tb09040.x.
[54] M. Słaba, P. Bernat, S. Rożalska, J. Nykiel, J. Długoński, Comparative study of metal induced phospholipid modifications in the heavy metal tolerant filamentous fungus Paecilomyces marquandii and implications for the fungal membrane integrity, Acta Biochim. Pol. 60 (2013) 695–700.
[55] M.F. Renne, A.I.P.M. de Kroon, The role of phospholipid molecular species in determining the physical properties of yeast membranes, FEBS Lett. 592 (2018) 1330–1345, https://doi.org/10.1002/1873-3468.12944.
[56] M.L. Gurr, J.P. Harwood. Lipid Biochemistry, fourth ed., Springer, 1991.
[57] ⟨https://avanti.com⟩.
[58] M. Sinensky, Homeoviscous adaptation - a homeostatic process that regulates the viscosity of membrane lipids in Escherichia coli, Proc. Natl. Acad. Sci. USA 71 (1971) 522–525, https://doi.org/10.1073/pnas.71.2.522.
[59] H.J. Heipieper, A.J.A.M. de Bont, Adaptation of Pseudomonas putida S12 to ethanol and toluene at the level of fatty acid composition of membranes, Appl. Environ. Microbiol. 60 (1994) 4440–4444, https://doi.org/10.1128/aem.60.12.4440-4444.1994.
[60] J.T. Davies, E.K. Rideal, Interfacial Phenomena, Academic Press, New York, 1961.
[61] P. Fontaine, G. Ciatto, N. Aubert, M. Goldmann, Soft interfaces and resonant investigation on undulation source: a surface X-ray scattering beamline to study organic molecular films at the SOLEIL synchrotron, Sci. Adv. Mater. 6 (2014) 2312–2316, https://doi.org/10.1166/sam.2014.2189.
[62] M.I. Angelova, D.S. Dimitrov, Liposome electroformation, Faraday Discuss. Chem. Soc. 81 (1986) 303–311, https://doi.org/10.1039/DC9868100303.
[63] M. Kang, C.A. Day, A.K. Kenworthy, E. DiBenedetto, Simplified equation to extract diffusion coefficients from confocal FRAP data, Traffic 13 (2012) 1589–1600, https://doi.org/10.1111/tra.12008.
[64] R.B. Lira, J. Steinkühler, R.L. Knorr, R. Dimova, K.A. Riske, Posing for a picture: vesicle immobilization in agarose gel, Sci. Rep. 6 (2016) 25254, https://doi.org/10.1038/srep25254.
[65] H.C. Ishikawa-Ankerhold, R. Ankerhold, G.P.C. Drummen, Advanced fluorescence microscopy techniques—FRAP, FLIP, FLAP, FRET and FLIM, Molecules 17 (2012) 4047–4132, https://doi.org/10.3390/molecules17044047.
[66] F. Pincet, V. Adrien, R. Yang, R, J. Delacotte, J.E. Rothman, W. Urbach, D. Tareste, FRAP to characterize molecular diffusion and interaction in various membrane environments, PLoS ONE 11 (2016) e0158457.
[67] R.S. Gracia, N. Bezlyepkina, R.L. Knorr, R. Lipowsky, R. Dimova, Effect of cholesterol on the rigidity of saturated and unsaturated membranes: fluctuation and electrodeformation analysis of giant vesicles, Soft Matter 6 (2010) 1472–1482, https://doi.org/10.1039/B920629A.
[68] H.A. Faizi, H.A, C.J. Reeves, V.N. Georgiev, P.M. Vlahovska, R. Dimova, Fluctuation spectroscopy of giant unilamellar vesicles using confocal and phase contrast microscopy, Soft Matter 16 (2020) 8996–9001, https://doi.org/10.1039/D0SM00943A.
[69] G. Brezesinski, A. Dietrich, B. Struth, C. Böhm, W.G. Bouwman, K. Kjaer, H. Möhwald, Influence of ether linkages on the structure of double-chain phospholipid monolayers, Chem. Phys. Lipids 76 (1995) 145–157.
[70] C.E. Miller, J. Majewski, E.B. Watkins, D.J. Mulder, T. Gog, T.L. Kuhl, Probing the local order of single phospholipid membranes using grazing incidence X-ray diffraction, Phys, Rev. Lett. 108 (2008) 058103 https://doi.org/0.1103/PhysRevLett.100.058103.
[71] K. Połeć, A. Wójcik, M. Flasiński, P. Wydro, M. Broniatowski, K. Hąc-Wydro, The influence of terpinen-4-ol and eucalyptol – the essential oil components - on fungi and plant sterol monolayers, Biochim. Biophys. Acta 1861 (2019) 1093–1102, https://doi.org/10.1016/j.bbamem.2019.03.015.
[72] K. Thirumoorthy, N. Nandi, D. Vollhardt, Role of dipolar interaction in the mesoscopic domains of phospholipid monolayers: dipalmitoylphosphatidylcholine and dipalmitoylphosphatidylethanolamine, Langmuir 23 (2007) 6991–6996, https://doi.org/10.1021/la070168z.
[73] A. Ivankin, L. Kuzmenko, D. Gidalevitz, Cholesterol-phospholipid interactions: new insights from surface X-ray scattering data, Phys. Rev. Lett. 104 (2010) 108101, https://doi.org/10.1103/PhysRevLett.104.108101.
[74] National Library of Medicine official site: https://pubchem.ncbi.nlm.nih.gov.
[75] S. Bose, P.S. Kumar, D.V.N. Vo, N. Rajamohan, R. Saravanan, Microbial degradation of recalcitrant pesticides: a review, Environ. Chem. Lett. 19 (2021) 3209–3228, https://doi.org/10.1007/s10311-021-01236-5.
[76] P. Matúš, P. Littera, B. Farkas, M. Urík, Review on performance of Aspergillus and Penicillium species in biodegradation of organochlorine and organophosphorus pesticides, Microorganisms 11 (2023) 1485, https://doi.org/10.3390/microorganisms11061485.
[77] N. Akhtar, M.A. Mannan, Mycoremediation: expunging environmental pollutants, Biotechnol. Rep. 26 (2020) e00452, https://doi.org/10.1016/j.btre.2020.e00452.
[78] A.S. Purnomo, R. Nawfa, F. Martak, K. Shimizu, I. Kamei, Biodegradation of aldrin and dieldrin by the white-rot fungus Pleurotus ostreatus, Curr. Microbiol. 74 (2017) 320–324, https://doi.org/10.1007/s00284-016-1184-8.

[79] P. Perczyk, M. Młyńczak, P. Wydro, M. Broniatowski, Persistent organic pollutants in model fungal membranes, Eff. Act. phospholipases, Biochim. Biophys. Acta 1864 (2022) 184018.
[80] Y.M. Cabidoche, R. Achard, P. Cattan, C. Clermont-Dauphin, F. Massat, J. Sansoulet, Long-term pollution by chlordecone of tropical volcanic soils in the French West Indies: a simple leaching model accounts for current residue, Environ. Pollut. 157 (2009) 1697–1705, https://doi.org/10.1016/j.envpol.2008.12.015.
[81] C. Merlin, M. Devers, O. Crouzet, C. Heraud, C. Steinberg, C. Mougin, F. Martin-Laurent, Characterization of chlordecone-tolerant fungal populations isolated from long-term polluted tropical volcanic soil in the French West Indies, 4914-1927, Environ. Sci. Pollut. Res. 21 (2014), https://doi.org/10.1007/s11356-013-1971-8.
[82] A. Wójcik, P. Perczyk, P. Wydro, M. Broniatowski, Incorporation of cyclodiene pesticides and their polar metabolites to model membranes of soil bacteria, J. Mol. Liq. 298 (2020) 112019, https://doi.org/10.1016/j.molliq.2019.112019.
[83] J.L. Kure, C.B. Andersen, T.E. Rasmussen, B.C. Lagerholm, E.C. Arnspang, Defining the diffusion in model membranes using line fluorescence recovery after photobleaching, Membranes 10 (2020) 434, https://doi.org/10.3390/membranes10120434.
[84] C. Fabiani, V.N. Georgiev, D.A. Penalva, L. Sigaut, L. Pietrasanta, J. Corradi, R. Dimova, S.S. Antollini, Membrane lipid organization and nicotinic acetylcholine receptor function: a two-way physiological relationship, Arch. Biochem. Biophys. 730 (2022) 109413, https://doi.org/10.1016/j.abb.2022.109413.
[85] R. Dimova, Recent developments in the field of bending rigidity measurements on membranes, Adv. Colloid Interface Sci. 208 (2014) 225–234, https://doi.org/10.1016/j.cis.2014.03.003.

Supplementary Materials to the article "Interactions of polychlorinated cyclodiene pesticides with model fungal membranes – Langmuir monolayer and liposome studies"

by Marcin Broniatowski and co-authors

Characterization of one-component Langmuir monolayers formed by the studied lipids

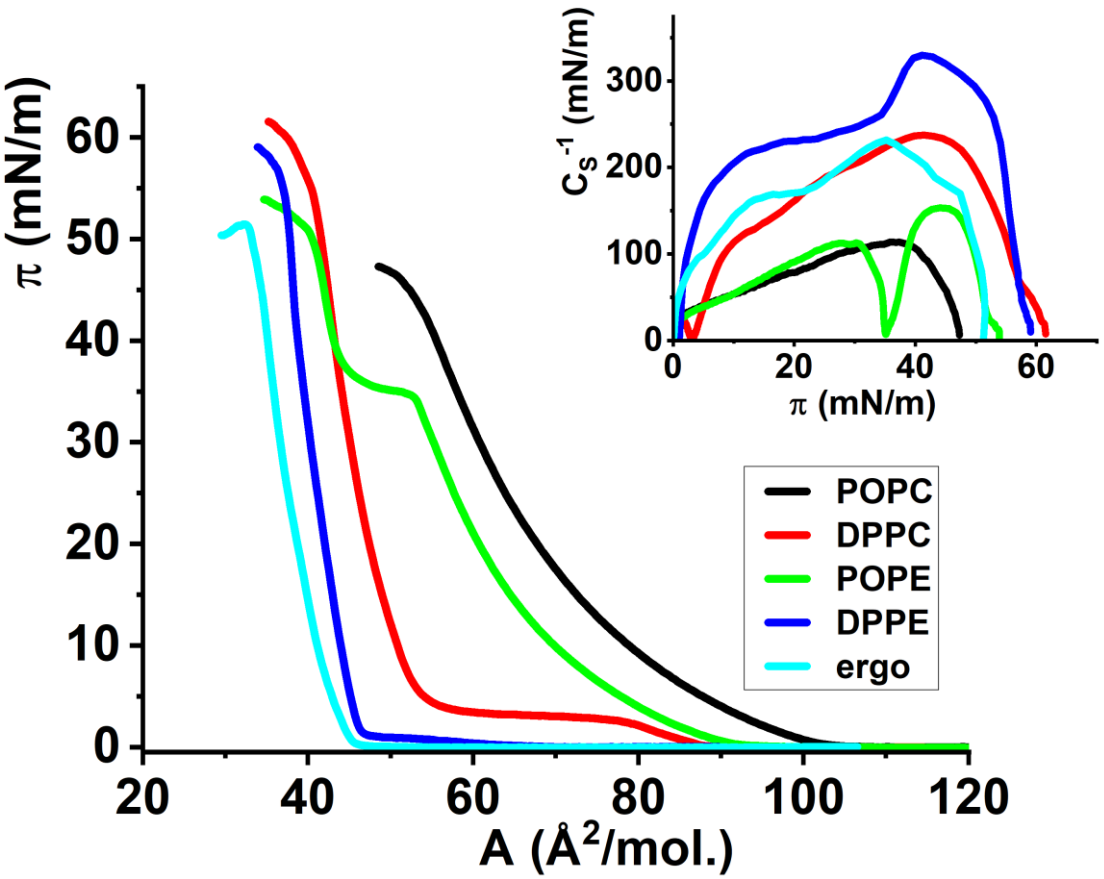

Figure S1. π-A isotherms and C_S^{-1}-π dependences for one-component Langmuir monolayers formed of the lipids employed in these studies.

Grazing Incidence X-ray Diffraction (GIXD) results for the MFS model membrane doped with the studied cyclodiene pesticides

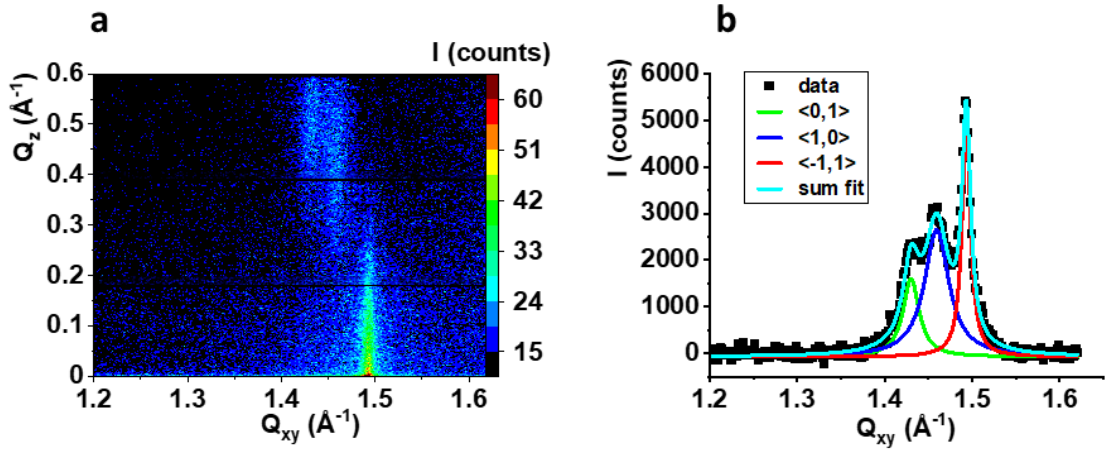

Figure S2. GIXD data for the MFS monolayer doped with aldrin, X(ALD) = 0.20, π = 20 mN/m. a) I(Q_{xy},Q_z) intensity map, b) Bragg peak integrated over all Q_z values, solid lines are Lorentz curves fit to the experimental data.

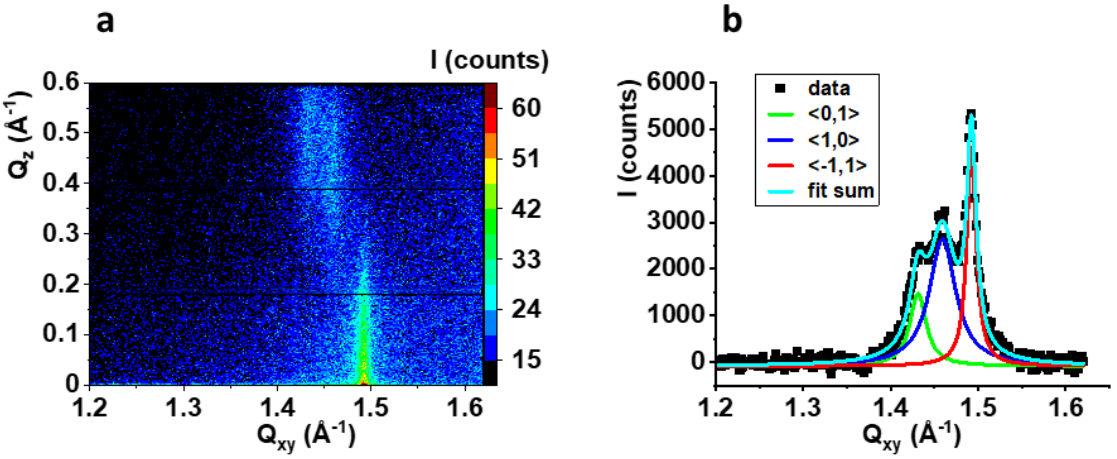

Figure S3. GIXD data for the MFS monolayer doped with endrin, X(END) = 0.20, π = 20 mN/m. a) I(Q_{xy},Q_z) intensity map, b) Bragg peak integrated over all Q_z values, solid lines are Lorentz curves fit to the experimental data.

Table S1 Structural parameters for the MFS monolayer doped in ALD and END

System	Q_{xy}, Q_z (Å^{-1}, Å^{-1})	Unit parameters a, b, γ (Å, Å, deg)	A (Å^2)	τ (deg)	Lxy (Å)
MFS+ALD	<0,1> 1.430, 0.51 <1,0> 1.459, 0.44 <-1,1> 1.493, 0.02	4.867, 4.966, 117.8	21.39	21.0	<0,1> 251±11 <1,0> 163±5 <-1,1> 461±10

MFS+END	<0,1> 1.431, 0.50 <1,0> 1.459, 0.43 <-1,1> 1.492, 0.02	4.870, 4.966, 117.8	21.38	20.3	<0,1> 240±21 <1,0> 149±8 <-1,1> 425±10

Where a, b, γ – lattice units, A_{xy} – area per one chain, τ – tilt angle of the hydrocarbon chains from the monolayer normal, L_{xy} – correlation distance within the crystalline domains.

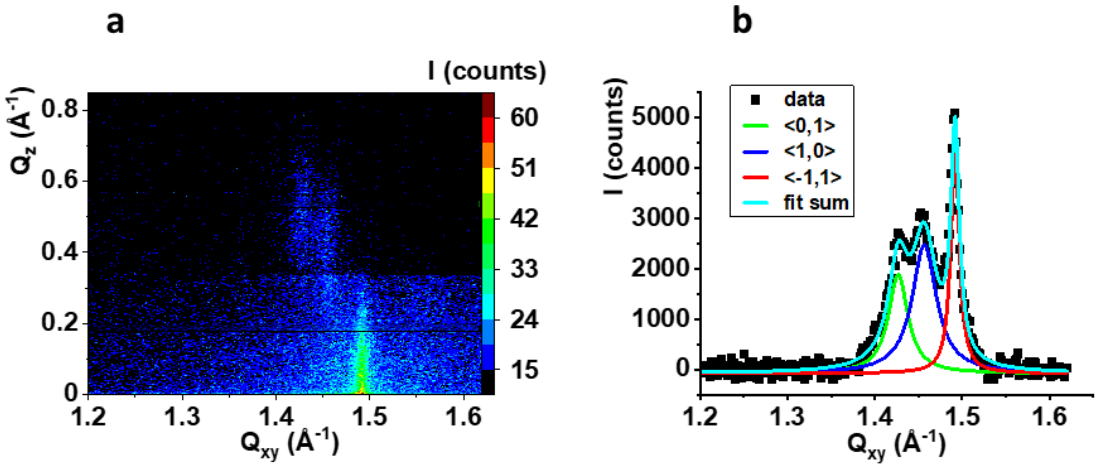

Figure S4. GIXD data for the MFS monolayer doped with endosulfan, X(EDS) = 0.20, π = 20 mN/m. a) I(Q_{xy},Q_z) intensity map, b) Bragg peak integrated over all Q_z values, solid lines are Lorentz curves fit to the experimental data.

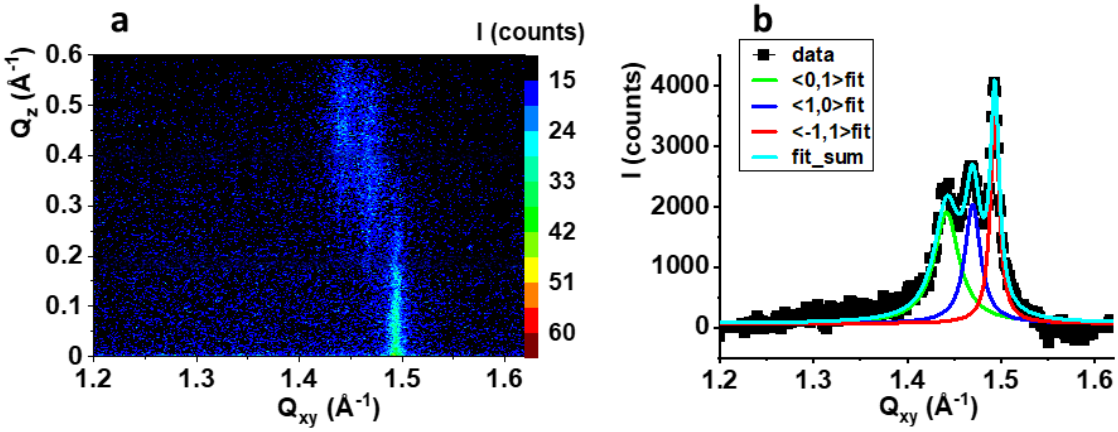

Figure S5. GIXD data for the MFS monolayer doped with chlordecone, X(CDN) = 0.20, π = 20 mN/m. a) I(Q_{xy},Q_z) intensity map, b) Bragg peak integrated over all Q_z values, solid lines are Lorentz curves fit to the experimental data.

Table S2. Structural parameters for the MFS monolayer doped in EDS and CDN

System	Q_{xy}, Q_z ($Å^{-1}$, $Å^{-1}$)	Unit parameters a, b, γ (Å, Å, deg)	A ($Å^2$)	τ (deg)	Lxy (Å)
MFS+EDS	<0,1> 1.427, 0.53 <1,0> 1.457, 0.42 <-1,1> 1.492, 0.02	4.871, 4.973, 117.7	21.45	21.3	<0,1> 205±15 <1,0> 163±10 <-1,1> 461±12
MFS+CDN	<0,1> 1.442, 0.51 <1,0> 1.461, 0.43 <-1,1> 1.493, 0.03	4.855, 4.950, 118.9	21.15	20.2	<0,1> 173±12 <1,0> 157±8 <-1,1> 429±15

Where a, b, γ – lattice units, A_{xy} – area per one chain, τ – tilt angle of the hydrocarbon chains from the monolayer normal, L_{xy} – correlation distance within the crystalline domains.

Initial characteristics of the LUVs after formation

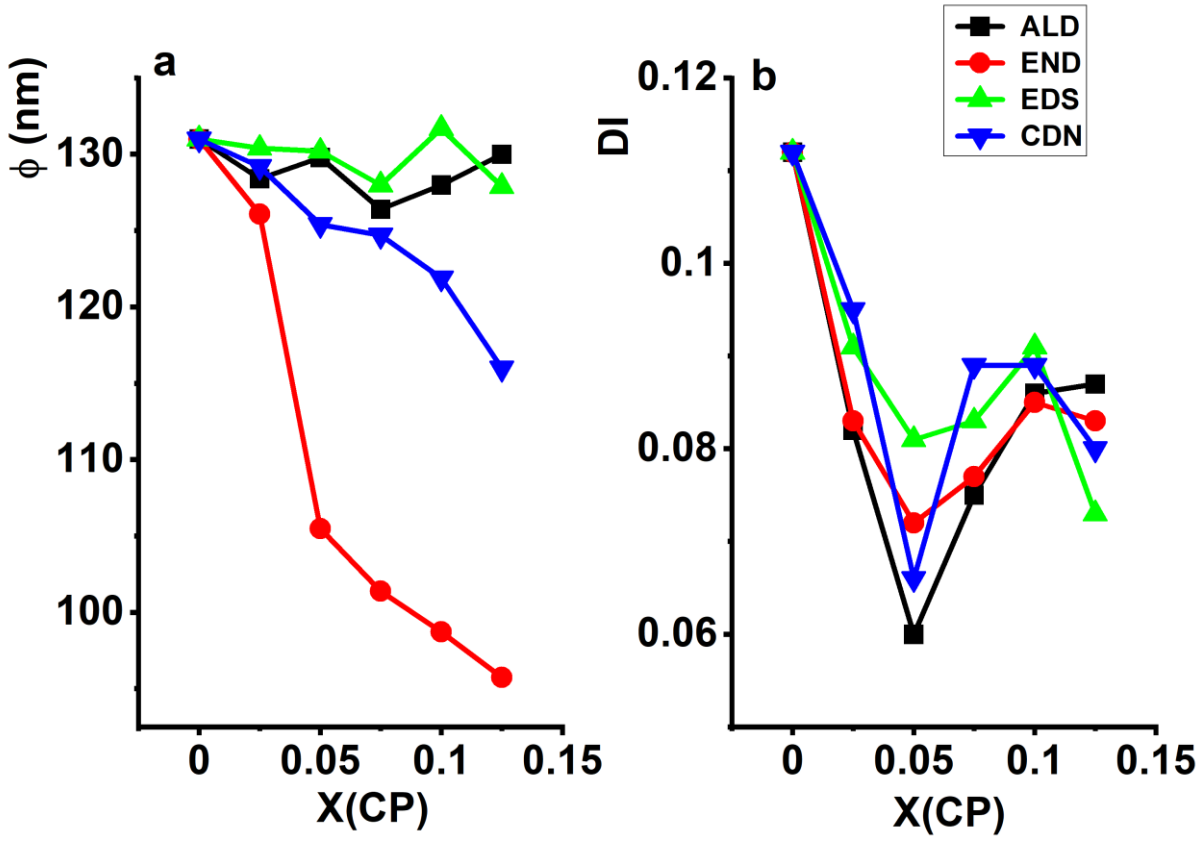

Figure S6. DLS characteristics of the LUV liposomes containing incorporated CP molecules. a) Hydrodynamic diameter φ, the experimental uncertainty is ± 2 nm b) polydispersity index DI